



Progressive Collapse Resistance of Bolted Extended End-Plate Moment Connections

Samad Barmaki¹ · Mohammad R. Sheidaii^{1,2}  · Omid Azizpour¹

Received: 15 August 2019 / Accepted: 15 April 2020 / Published online: 24 April 2020
© Korean Society of Steel Construction 2020

Abstract

When a progressive collapse occurs due to sudden column removal, the moment connections must have adequate strength and be able to bridge over the damaged element. The present study comprehensively investigates the behavior of eight different types of extended end-plate beam-to-column connections against progressive collapse. The proper finite element models have been extended to assess the behavior of these bolted connections under a sudden column removal scenario. Specimens were checked by nonlinear analysis method. The fracture modes, Von-Mises stresses, vertical load–displacement and load factor–displacement curves, load transfer mechanisms, and other analytical results comparative were reported in detail and discussed for various investigated beam-to-column connections. The analysis results revealed that the overall failure of the samples occurred in the connection region under the catenary action mode at large displacements. Also, the results were verified with available experimental data. Among all investigated connections, the highest stresses could be applied to the sixteen-bolt stiffened connection, and this sample had the most excellent behavior. In the design of buildings exposed to unusual loads due to progressive collapse, the significant axial force created in the connections should be considered in the design stages of these elements. Also, it is recommended that at least three rows of bolts are embedded in the bottom area of end-plate connections when the structure is at the risk of progressive collapse.

Keywords Beam-to-column connection · Progressive collapse · Nonlinear analysis · Finite element model · Bolted end-plate connection · Catenary action

1 Introduction

One of the most significant concerns in the design of projects is structural safety. In recent decades, progressive collapse as one of the failure modes of structures has attracted much attention (Ch-Salmasi and Sheidaii 2017). "Progressive collapse is defined as the spread of an initial local failure from element to element, eventually resulting in the collapse of the entire structure or a disproportionately large part of it" (ACSE 2016). Progressive collapse is a phenomenon where abnormal loads cause local damage, and the structure distorts the damage due to lack of continuity, ductility, and indeterminacy. If the structure has sufficient continuity and

ductility against the development of progressive collapse, only local collapse occurs in the structure. In many progressive collapse events, it has been observed that the casualties in the structural failure are far higher than those occurring during the initial abnormal load on the structure (Astaneh-Asl et al. 2001).

For the first time, the centralization of the engineering society expressed in progressive collapse via the failure of a part of the Ronan Point building in 1968. (Zhong et al. 2017). More attention was paid to the structural response to unexpected accidents after the collapse of the WTC in 2001 (NIST 2005). The occurrence of progressive collapse can lead to catastrophic outcomes in the structures. Thus, the control criteria of the buildings against this event have gradually been incorporated in design guidelines. Rethinking and modifying the standards for the design phase of anti-progressive collapse has attracted the attention of many researchers. Comprehensive studies in this field have been conducted by the US Department of Defense (DoD) and the UFC (2016) and GSA (2013). The alternate load path method (APM),

✉ Mohammad R. Sheidaii
m.sheidaii@urmia.ac.ir

¹ Department of Civil Engineering, Urmia Branch, Islamic Azad University, Urmia, Iran

² Department of Civil Engineering, Urmia University, Urmia, Iran

an influential approach to decreasing the risk of progressive collapse, has been mentioned in GSA and UFC guidelines. A schematic example is exhibited in Fig. 1a when a central column has been damaged by an abnormal load.

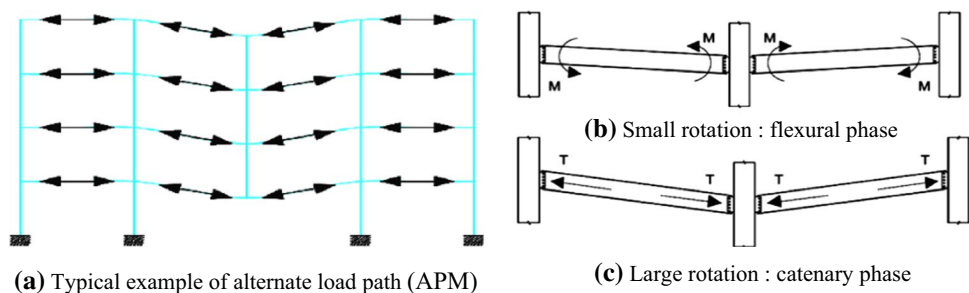
Typically, beam-to-column connections in a moment-resisting frame are designed to withstand normal gravity and seismic loads. Specifically, the failure of connections and internal actions created in these frames to confront the load caused by an earthquake is different from the behavior of these connections against the progressive collapse resulting from sudden column removal. The primary expectation of the moment frame design is to prevent connection failure to achieve a ductile structural behavior. The performances of the members demonstrated in Fig. 1 show that they are rotation-dependent. After a specific value of rotation, a significant axial force appears in the beam and connections at large rotations in the catenary action mode, as displayed in Fig. 1c (Daneshvar 2013). In this case, a large tensile axial force appears in the connections, making its behavior different from the seismic situation. In other words, if a moment frame is appropriately designed for seismic loads, there is no certainty that the structure will resist the progressive collapse, since the internal forces and, thus, the type of connection behavior are different in these two situations. For example, a considerable axial force can develop in the connections when the progressive collapse occurs, making their failure behavior very different.

Beam-to-column connections have an essential duty in resistance to gravity loads in the vicinity of a damaged column. The assessment of connections performance corresponding to the force transfer is principal in evaluating structural resistance against progressive collapse (Brett and Lu 2013). Analytical and experimental studies have been conducted by many researchers to understand the behavior of force transfer through connections. For example, Sadek et al. (2011) carried out an analytical and experimental evaluation of the behavior of reinforced concrete and steel moment frames against progressive collapse. The investigated structural systems of a 10-story building were IMFs and SMFs. The analysis results exhibited a similar fracture mechanism in the samples. The fracture of samples occurred at the bottom-flanges of beam. Fang et al. (2012) examined

the realistic performance of a multi-story car park under a vehicle fire scenario occurring near an internal column. In their study, the emphasis was given to the robustness and ductility response of the floor systems after column buckling. The steel flush end-plate connection was selected for their study. The analysis results indicated that the actual ductility demands fall between two idealized extreme cases, called "static column loss" and "sudden column loss" Fang et al. (2013). developed a temperature-independent approach framework for the practical design-oriented robustness assessment of multi-story steel/composite structures against localized fire which is event-independent. The results showed that under the Temperature-Independent Approach (TIA) assessment framework, the reference building had generally sound robustness against localized fire. Lew et al. (2013) and Sadek et al. (2013) evaluated the behavior of two types of fully restrained beam-to-column connection against progressive collapse. They evaluated the performance of two rigid connections: (1) WUF-B and (2) RBS. They found that the connections could support significant axial forces, and therefore were able to withstand the gravity loads applied via the catenary action mode. Yang and Tan (2012a, b) analyzed the performance of various bolted, beam-to-column simple, and semi-rigid connections. For this purpose, the behavior of seven conventional beam-to-column connection was investigated with the experimental tests against progressive collapse. This study provided the failure mechanism and behavior of various connections including their abilities to distort in the catenary action phenomenon. The analysis results indicated that component-based models should be considered for designing structures against progressive collapse.

Li et al. (2013, 2015) analyzed the robustness and failure mode of several types of steel moment connections against progressive collapse. The analysis results showed that the samples primarily resisted the load applied by flexural action in the initial stage. With increasing vertical-displacement, the bearing-load mechanism progressively shifted towards relying on the catenary action mode. Qin et al. (2015, 2016) performed an analytical and experimental assessment on the behavior of a reinforced welded flange-bolted web connection and a conventional welded flange-bolted web

Fig. 1 Formation of catenary behavior in beams (Daneshvar 2013)



connection against progressive collapse. They found that the strength and deformability of reinforced flange-bolted connection were better than any other connections. Meng et al. (2018) investigated the performance of various types of connections including two beams and three columns against progressive collapse. They evaluated the behavior of three different samples with WUF-B beam-to-column connection with distinct span ratios of 1:1.4, 1:1.0, and 1:0.6. The analysis results indicated that the span ratio of 1:1.0 outperformed other span ratios against progressive collapse. Also, the load transfer of specimens with equal spans was more desirable than that of samples with nonequal span ratios.

A review of the literature suggests that the performance of bolted beam-to-column connections against progressive collapse has been assessed by only an insignificant number of studies. A considerable number of the research published have focused on the welded beam-to-column connections. In design guidelines of prequalified connections, bolted steel connections such as double-tee, bolted flange plate, extended end-plate, and Kaiser bolted bracket are typical and these sets of connections while being subjected to column removal should be assessed. Hence, the present research examined the progressive collapse resistance of double full-span specimens with various bolted beam-to-column connections comprehensively against progressive collapse. Specifically, under a column removal scenario, the influences of connections performance were evaluated on the global behavior of the specimens. The specimens were checked by nonlinear analysis method. The fracture modes, Von-Mises stresses, vertical load–displacement and load factor–displacement curves, load transfer mechanisms, and other analytical results comparative were reported in detail and discussed for various investigated beam-to-column connections.

2 Finite Element (FE) Modeling

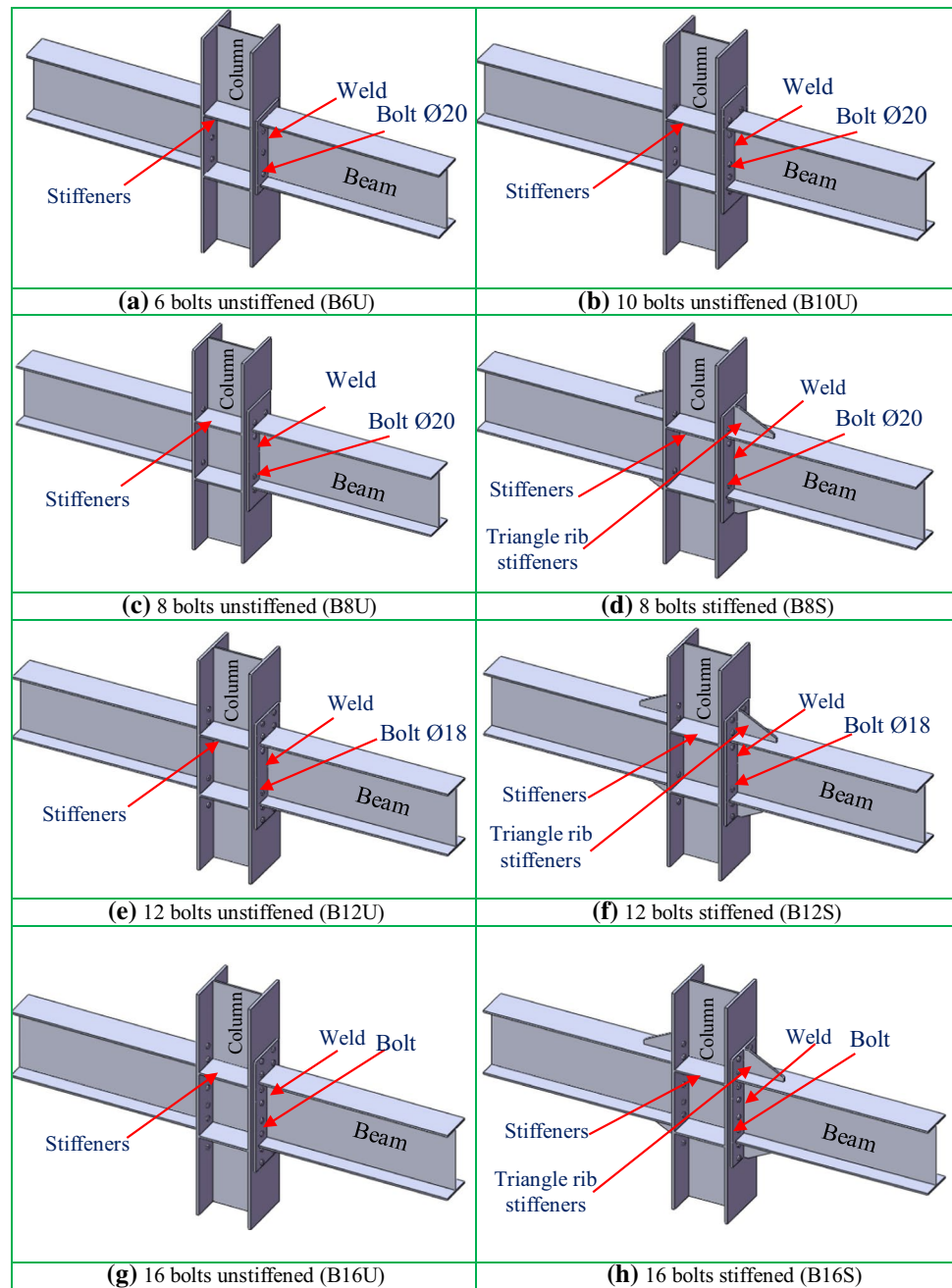
This study presents numerical simulations and analytical investigations of progressive collapse performance of bolted steel beam-to-column connections. The design of the beams, columns, and connections was in accordance with the seismic design regulation of AISC 360 (2016b), AISC 341 (2016a), and AISC 358 (2016c), respectively. The rigid bolted steel beam-to-column connections are one of the most common connections between rigid connections. In this connection, the beam is welded to a steel plate, and the steel plate is attached to the column flanges using bolts. In this research, eight different types of extended end-plate moment connections were chosen, as shown in Fig. 2. The high-strength bolts (Grade 10.9) with the size of M16, M18, and M20 were used for the specimens. Figure 3 demonstrates the investigated sample which is a separate part of an office structure. The lateral load-bearing system has been designed

in the form of a moment-resisting frame. AISC 341 (2016a) and AISC 360 (2016b) have been used for the design of steel elements, while the connections were designed according to the AISC 358 (2016c) regulations. Design gravity and seismic loads were calculated based on ASCE7 (2016) guidelines; the design spectral acceleration parameters S_s and S_1 were 0.81 g and 0.38 g, respectively. These structures were residential and are located in an area of moderate seismicity. These buildings were symmetrically designed in two main directions of the plan, with four spans. Each span was 6 m long. The number of stories in analytical models was equal to six. The height of the stories in all models was 3.5 m. The progressive collapse behavior of specimens was evaluated by applying increasing vertical-displacement at the top of the middle removed column, with the catenary action effects investigated in the adjacent elements. During the analysis stage, the gravity displacement of the failed column increased until the ultimate load-carrying capacity of assemblies was obtained. In this case, the connections were affected by combined tension and bending.

Once a central column was suddenly removed, the structure was divided into related and unrelated spans according to the APM in UFC (2016) guideline as depicted in Fig. 3. The related spans were recognized as the primary research zone in the damaged structures. To evaluate the behavior of the related spans under a central-column-removal scenario, a double full-span specimen with a failed column in the assembly center and two vicinity beams was modeled, as shown in Fig. 3a (Zhong et al. 2017). Figure 3b demonstrates the typical FE model of the sample structure. According to Fig. 3b, the vertical loading imposed on the remaining structure has been centered on the top of the removed column. At the inflection points, the horizontal and vertical hinge supports were selected for boundary conditions of the side columns, as shown in Fig. 3. The length L_c of the side column in Fig. 3a was considered to be 1100 mm. In the analysis conducted, the damaged column could only move in the vertical direction. The axial restraints from the adjacent beams and diaphragms were considered, and out-of-plane movements of the affected beams were constrained by defining the appropriate axial constraints at the end nodes of the beam element. Figure 4 displays the complete details of the 3D analytical model and schematic shape of eight specimens, bolt and nut.

In this research, the explicit time integration method in the ABAQUS (2014), a FE software package, was chosen for analyses of samples against progressive collapse. The push-down analysis with displacement-controlled loading was applied to all models with the damaged column being suddenly removed from the theoretical structural model. Displacements were continuously heightened until the fracture occurred. A vertical load combination of $1.2DL + 0.5LL$, as specified in the ASCE 7 (2016) and UFC (2016) guidelines,

Fig. 2 Analytical beam-to-column bolted unstiffened and stiffened extended end-plate moment connections

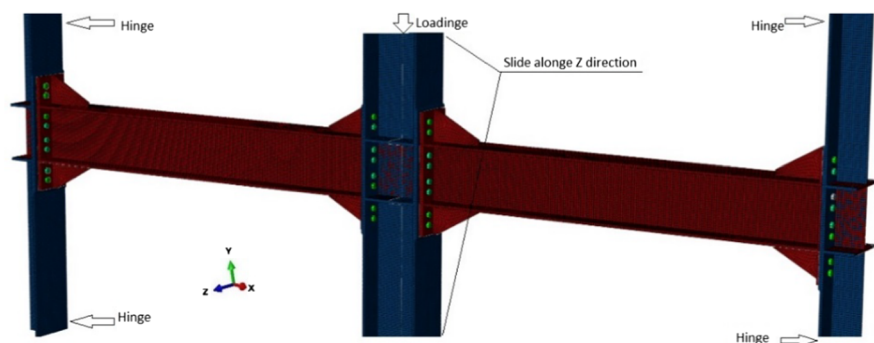
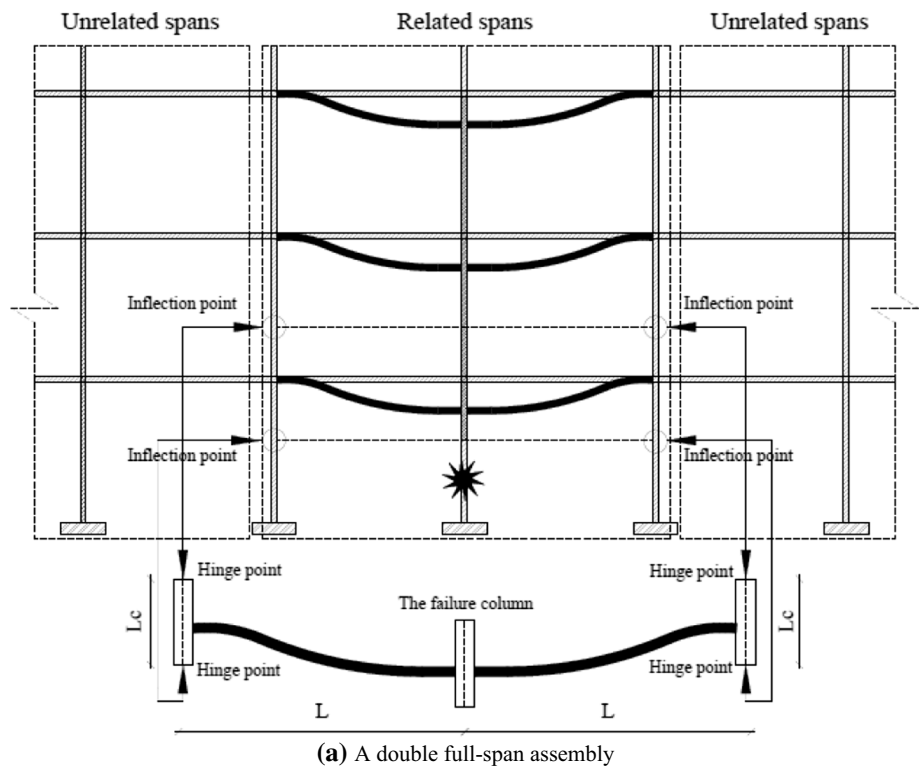


was applied. The concentrated column vertical forces were determined, and finally, the load factor for each connection was evaluated. Accordingly, in this case, the value calculated for the entire gravity load proposed by UFC guideline was 178 kN.

Comparisons between the analysis results of the detailed and the experimental results have been presented to validate the models developed herein. As proposed by Yang and Tan (2012a, b), provided that kinetic energy was maintained within 10% of internal energy, the explicit solver was used to the theoretical analysis of this research. The solid element of C3D8R in the ABAQUS element library was employed to

generate the entire model. As schematically shown in Fig. 5, a mesh size of 4 mm was selected for the beam and column elements, while a mesh size of 2 mm was chosen for the regions near the connection area. The general contacts were defined for the end-plate, webs, and bolts. "Hard contact" was applied to every contact pair. The isotropic Coulomb model, with a friction coefficient equal to 0.3, was utilized for steel-to-steel contacts. As no weld fracture occurred during the previous experimental tests, in this study, "tie" contact interaction was used between the end-plate and the beam flange. S355 steel was utilized for the beam and columns, respectively, with the Poisson's ratio of 0.3. The types and

Fig. 3 Beam-to-column assembly extracted from the steel frame



details of specimens as well as the material properties were obtained via coupon tests as summarized in Tables 1 and 2, respectively. The coupon tensile tests were employed based on the ASTM A370 (2018).

Ductile criterion Appropriate for triggering damage is due to nucleation, growth, and coalescence of voids. In the ABAQUS (2014), the model assumes that the equivalent plastic strain at the onset of damage is a function of stress triaxiality and strain rate. Regarding the non-uniform effect of increasing the equivalent plastic strain affected by the stress triaxiality growth, three dependent parameters were taken into account for the isotropic materials in the ABAQUS software.

In order to model the connections, the failure mode of progressive collapse was defined as Fig. 6. This kind of modeling removes the failed elements from the overall

meshing of the sample model. Meanwhile, the ductile and shear criteria in combination with the damage evolution models were used in modeling the fracture of ductile metals in ABAQUS software. In this research, the fracture strain properties based on the tri-axial stress and the strain rate of steel material were used to define the ductile criteria. Also, the fracture strain properties based on the shear stress ratio and the strain rate of steel material were utilized to determine the shear criteria in the modeling, with the value of K_s of steel considered as 0.03 in shear criterion.

In the solid elements of specimens, the approach to developing the material model parameters, including true stress vs. plastic strain for each steel type, was as follows:

- The true stress σ_T is based on the load divided by the actual cross-section area of the sample and is equal to

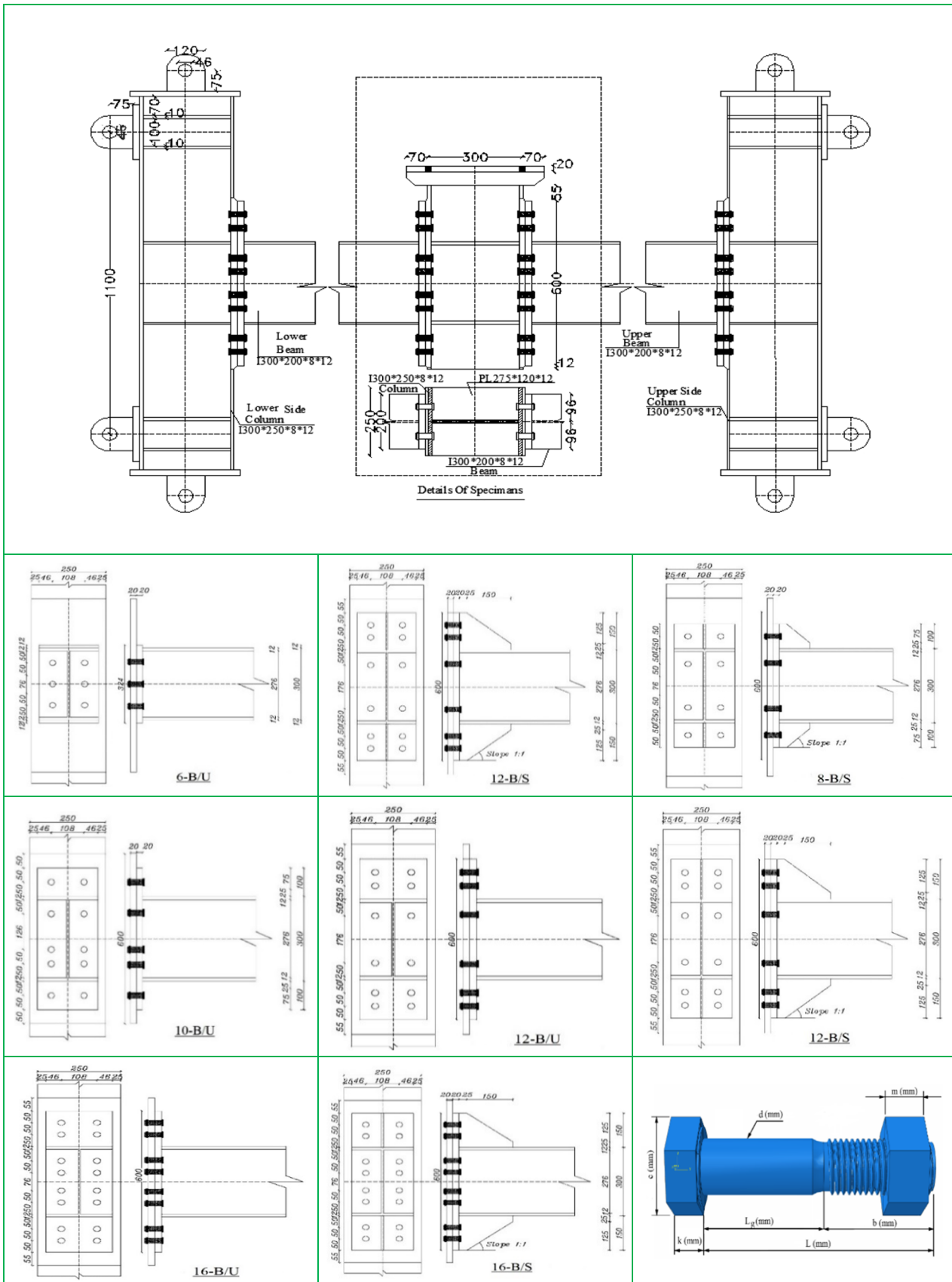


Fig. 4 Details of samples

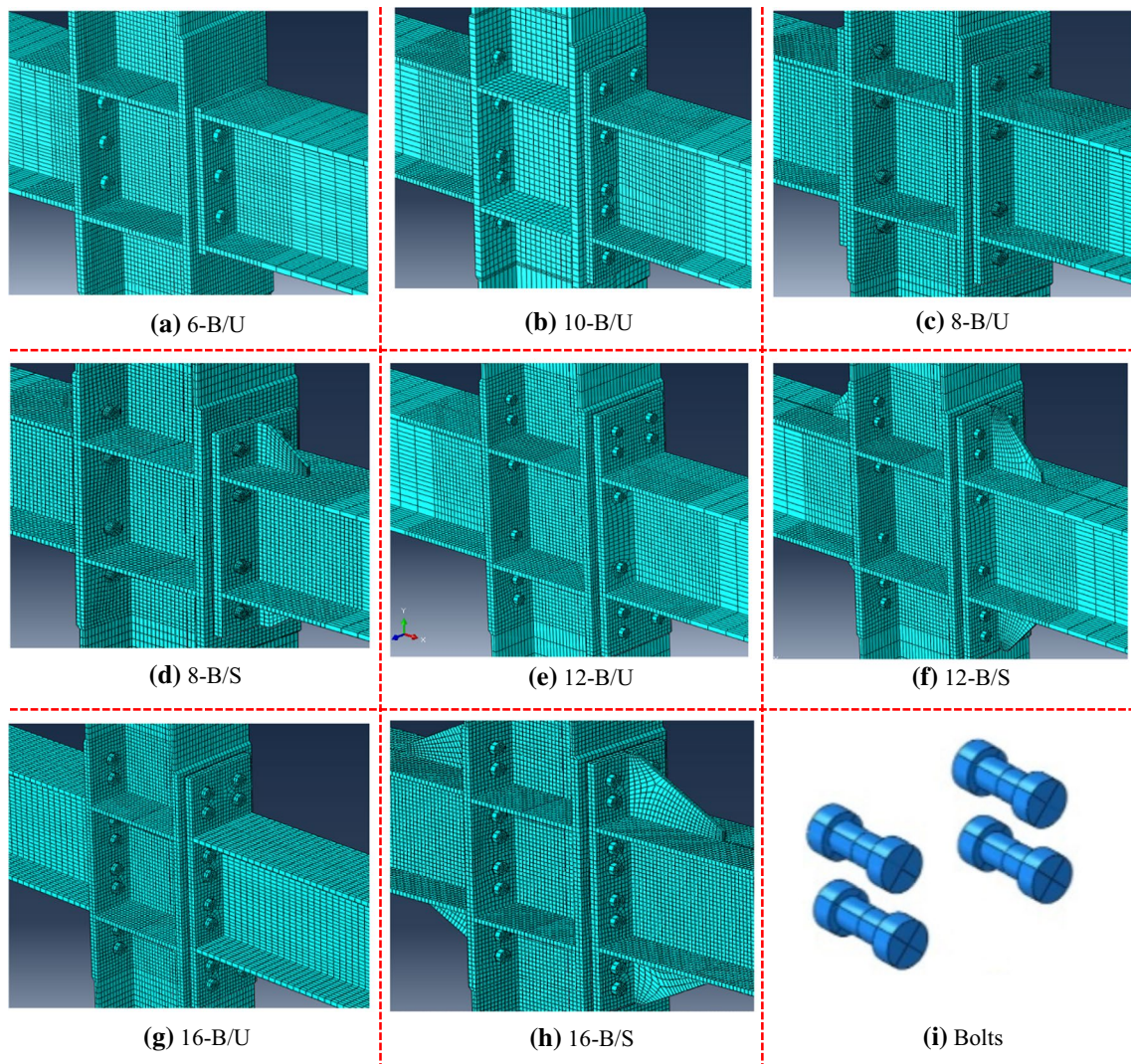


Fig. 5 Typical finite element model, meshing scheme and bolt samples

Table 1 Types and details of specimens

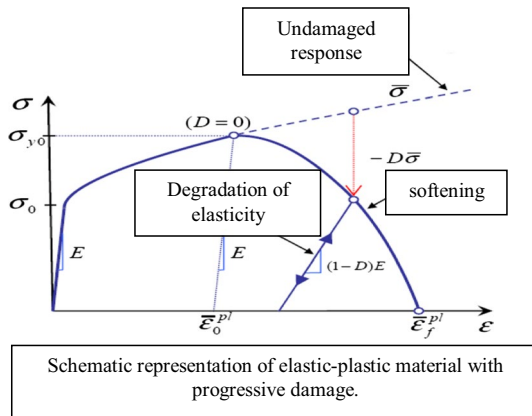
NO	Specimen	Abbreviated name	Details				
			Extended con- nection	Bolt diameter (mm)	Number of bolts	End-plate stiffener	Prequalified connections
1	Six-Bolt Unstiffened	6-B/U	No	20	6	No	No
2	Eight-Bolt Unstiffened	8-B/U	Yes	20	8	No	Yes
3	Eight-Bolt Stiffened	8-B/S	Yes	20	8	Yes	Yes
4	Ten-Bolt Unstiffened	10-B/U	Yes	20	10	No	No
5	Twelve-Bolt Unstiffened	12-B/U	Yes	18	12	No	Yes
6	Twelve-Bolt Stiffened	12-B/S	Yes	18	12	Yes	Yes
7	Sixteen-Bolt Unstiffened	16-B/U	Yes	16	16	No	Yes
8	Sixteen-Bolt stiffened	16-B/S	Yes	16	16	Yes	Yes

engineering stress σ_{eng} multiplied by a term to correct for the change in the cross-section (Eq. (1)):

$$\sigma_T = \sigma_{eng}(1 + \epsilon_{eng}) \tag{1}$$

Table 2 Material properties of the steel specimens

Component	Element	Material			
		Measured average yield strength (MPa)	Measured average tensile Strength (MPa)	Measured average elastic modulus (GPa)	Measured bolt average pretension force (kN)
Beam, column and connection	Thickness ≥ 16 mm	355	536.60	195.452	–
	Thickness < 16 mm	355	537	188.671	–
Bolts (10.9)	All bolt size	900	1160	204.277	199

**Fig. 6** Schematic representation of elastic–plastic material with progressive damage

Before the onset of localization (necking), the natural or true strain ε_T is defined as Eq. (2):

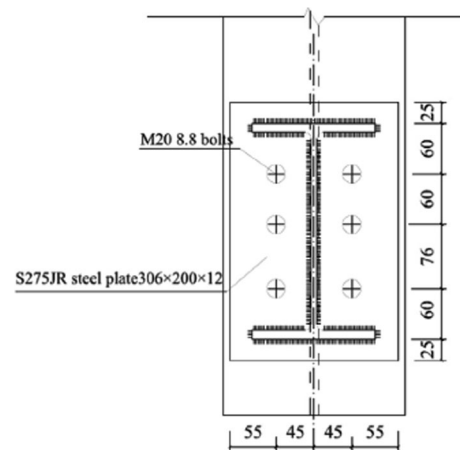
$$\varepsilon_T = \ln (1 + \varepsilon_{eng}) \quad (2)$$

- The plastic strain is then obtained as $\varepsilon_p = \varepsilon_T - \sigma_T/E$, where E is the Young's modulus, and σ_T/E represents the elastic strain.

3 Verification Results

Yang and Tan (2013) performed experimental tests on seven types of typical bolted beam-to-column connections against progressive collapse. The considered connections were simple and semi-rigid types. In their study, the performance and fracture modes of various connections were investigated by considering their ability to develop the catenary action mode.

In the current study, to validate the results of the simulations, Yang's sample structure with the flush end plate connection was modeled in ABAQUS software according to Fig. 7. The behavior of this connection was determined

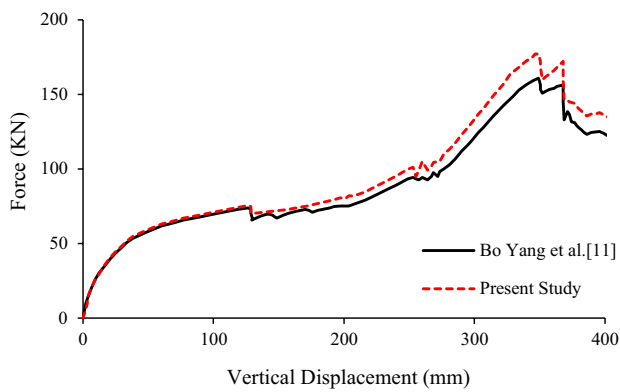
**Fig. 7** Details of the specimen with flush end plate connection

under the sudden column removal via dynamic explicit analysis.

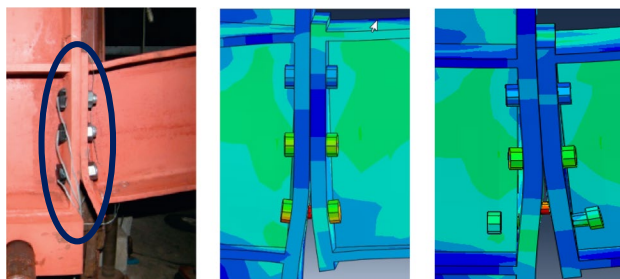
The diagram of vertical displacement–force, alongside the flush end plate connection failure in the main structure, examined by Yang and Tan (2013), is illustrated in Fig. 8 in a model that was remodeled by the author to be validated. According to Fig. 8, the analysis results have been consistent with the results in the current paper. According to Fig. 8b, the failure mode of the specimens has also been an exemplified of validation of the present study results.

4 Analysis Results

In the current study, numerical simulations were conducted, and the failure mode of all specimens was investigated under large deformations in different beam-to-column connection zones. To evaluate the strength of different connections against progressive collapse, a quasi-static nonlinear analysis with the displacement-controlled method was performed under the column removal in sample structures. Also, the gradual increase of the applied loads was analyzed on the structural models according to the proposed procedure. Based on previous research (Yang and Tan 2013; Sadek et al. 2010, 2011; Li et al.



(a) Vertical displacement - force



(b) Failure mode of the flush end plate connection

Fig. 8 Vertical force–displacement curve and FE results for the specimen with flush end plate connection

2013; Wang et al. 2016), a three-dimensional finite element model was employed for the modeling and analysis as well as for estimating the vulnerability of sample models under a central-column-removal scenario.

Next, the results of the progressive collapse analysis of the sample model with a 12-B/U connection are presented in detail. Then, the comparison diagrams of the column removal results from the sample structure have been demonstrated and discussed for the other connection samples.

4.1 Results of Moment Frame with the 12-B/U Connection Under the Column Removal

For a quasi-static nonlinear analysis in the model with 12-B/U connection, initially, the diagram of the vertical displacement-force and load factor-displacement of the structure under the column removal has been plotted in Fig. 9. Then, the stress at different points of the section and the failure modes are illustrated in Fig. 10 to determine the susceptibility of the structure with the 12-B/U beam-to-column connection. Note that the displacement of these diagrams implies the gravity displacement at the top of the removed column. In the current analysis of progressive collapse, the ratio of the gravity load applied in each step of the quasi-static nonlinear analysis to the entire gravity load proposed by UFC guideline is called load factor.

According to Fig. 9, At an intermediate moment, resisting frame with the beam-to-column connection of type 12-B/U, and displacement less than 10.33 cm at point A1, the linear behavior of load–displacement is shown in the sample structure. It indicates the elastic flexure behavior in the initial stages of loading. At this point, according to Fig. 10a, the stresses due to the tension and compression of internal elastic bending force have been concentrated in the bottom and top flanges of beam, respectively. From point A2, at the vertical force of 170.11 kN and the equivalent load factor of 0.96, the sample enters the nonlinear region of materials with the slope of the load–displacement diminished. As shown in Fig. 10b, at this point, the focus of the principal stresses in the ended plate occurred along the bottom-flange of beam. As the displacement increased from A2 to A3 and with the transition from small deformations to large structural deformations, the reaction of the structure changed from the bending phase to the catenary phase. Thus, the catenary action has appeared in the connection. In this stage, a considerable axial tension force develops in the sample and affects the bottom half of the beam, as observed in Fig. 10c. As shown in Fig. 9 at point A4, the structure has been able to withstand the progressive collapse vertical load of 241.46

Fig. 9 The vertical load–displacement curve of 12-B/U sample

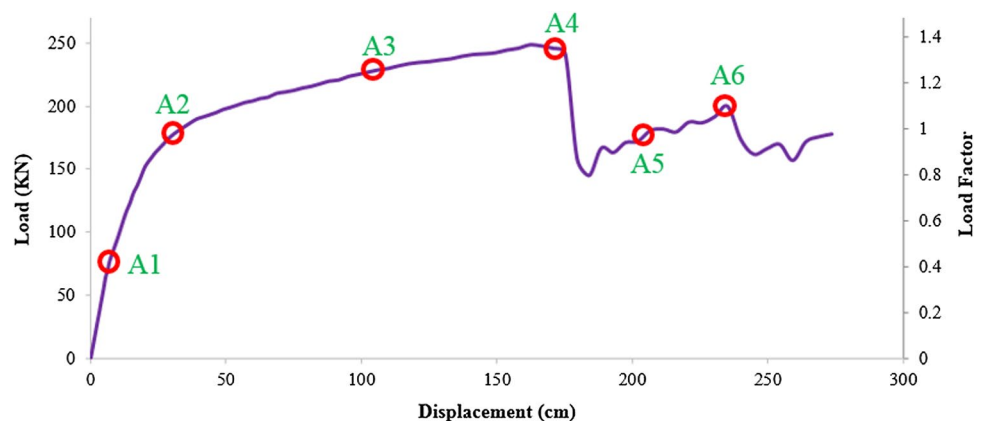
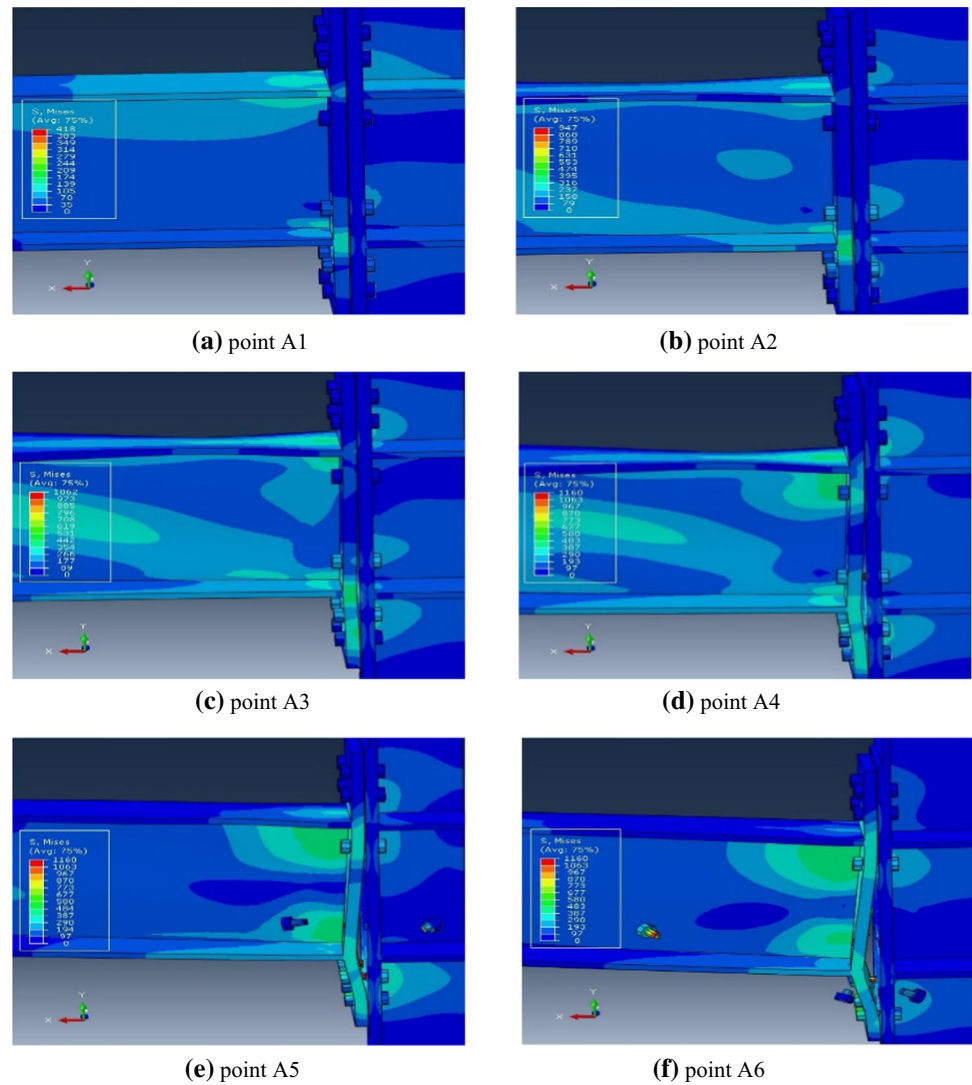


Fig. 10 Step by step collapse results of the 12-B/U sample



kN corresponding to a load factor of 1.36. The displacement of the top node of the removed column in the maximum load factor has been 17.52 cm. In this stage, based on Fig. 10d, the body of two rows of bolts located near the bottom-flange of beam has reached critical stresses under the tensile applied force to the sample structure. One of the mid-bolts fractured near the beam flange, after which a sharp drop occurred in the strength. Because of that, the maximum bearing load factor in this sample has been larger than unity; the 12-B/U connection is sufficiently resistant against progressive collapse. As the displacement-control analysis continued, at point A5, the web stresses of the beam near the flanges increased; according to Fig. 10e, the bolts located along the web direction and around the bottom-flange of beam fractured one after the other. The stress concentration and the shear fracture due to shear band localization cause fracture of bolts. Finally, at the displacement of 23.51 cm and a load factor of 0.74, at point A6, the majority of the bolts were broken and the overall fracture occurred in the

connection, as shown in Fig. 10f. Hence, as a general result, it can be stated that during the occurrence of progressive collapse, the concentration of principal stresses occurs in the bottom-flange of beam. By strengthening this region of connection, the total resistance of the system against progressive collapse can be significantly enhanced.

4.2 Results of Moment Frame with Various Types of Connection Under the Column Removal

The sample structure with six types of prequalified connections, a proposed connection, and an experimental sample was modeled as finite elements in full detail and analyzed further against progressive collapse under the single column removal. The diagrams of vertical displacement–force, load factor–displacement, and stress at various points of the cross-section and different failure modes have been shown to determine the structure susceptibility in every connection under the sudden column removal. Comparison of the

diagrams of vertical displacement–force and load factor–displacement of the sample structure in the beam-to-column connection is shown in Fig. 11 for eight various types of connection. If the ductility coefficient is taken as the ratio of the displacement corresponding to the maximum load factor on the displacement corresponding to the yield limit of the sample, the 16-B/S connection has the best strength and ductility behavior compared to the other connections with the load factor of 2.21 and ductility of 8.89. The 6-B/U connection with the load factor of 0.57 and ductility of 3.06 showed an undesirable strength performance. Since the load factor of the 6-B/U and 8-B/U connections has been smaller than unity, these connections are not sufficiently resistant against progressive collapse and did not indicate a proper behavior. However, six other connections with a load factor greater than unity demonstrated a desirable resistance against progressive collapse.

Table 3 summarizes the results of eight connections under the sudden column removal. According to Table 3, it is

deduced that the installation of stiffener in the beam flanges as well as the consideration of the number of more bolts at the end-plate connections will make the performance more efficient and absorb more energy from the connection against progressive collapse. Further, as the load factor increased, so did the safety factor of structure against progressive collapse. Meanwhile, by looking carefully at the 10-B/U connection behavior compared to the 8-B/U connection, it was seen that by adding a row of bolts near the bottom-flange of beam, with this element placed under a significant axial tension force in the catenary phase, the load factor increased from 0.89 to 1.29, with this change practically making the sample resistant to progressive collapse. This can be attributed to increased resistance against the prying action due to the growing number of bolts' row of the tensile stress area. Thus, in structures with the occurrence probability of progressive collapse, it is recommended that an end-plate connection is considered with the stiffener; alternatively, in the vicinity of the bottom-flange of beam, it is necessary to

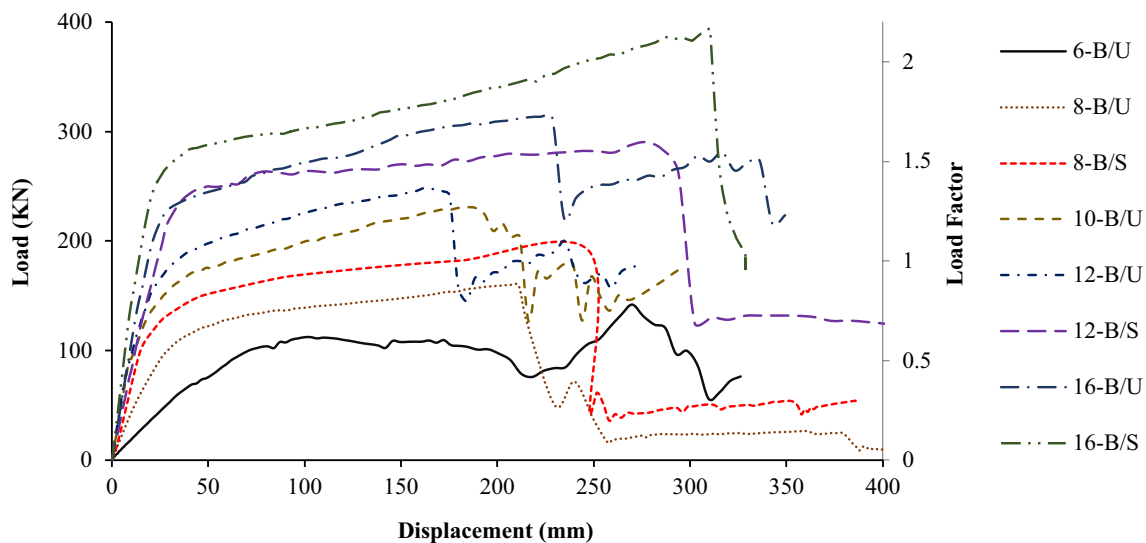


Fig. 11 Vertical load–displacement curve and load factor–displacement of the different connections

Table 3 Results summary of the various connections under the column removal

No	Connection type	Load factor of yielding limit	Maximum load factor	Ultimate load (kN)	Yielding displacement (cm)	Ultimate displacement (cm)	Ductility
1	6-B/U	0.35	0.57	102.97	3.67	11.23	3.06
2	8-B/U	0.60	0.89	159.13	3.30	21.11	6.40
3	8-B/S	0.78	1.12	199.69	3.52	23.52	6.68
4	10-B/U	0.91	1.29	230.16	2.41	18.87	7.83
5	12-B/U	1.01	1.39	247.49	3.28	16.65	5.08
6	12-B/S	1.34	1.63	290.28	4.08	27.69	6.78
7	16-B/U	1.24	1.76	313.28	2.63	22.85	8.69
8	16-B/S	1.54	2.21	394.39	3.49	31.03	8.89

install three rows of bolts in the design stage. The analysis results also demonstrated that in the end-plate connections without changing the number and size of bolts, the installation of stiffener can significantly increase the structural capacity and resistance against the prying action, in order to improve the performance of the structure against progressive collapse in some cases.

Figure 10 depicts the performance of the sample structure with the 12-B/U connection. Also, the behavior of seven other connections against the sudden column removal is briefly summarized in the most important steps of the analysis including (a) yielding, (b) ultimate load, (c) fracture, and (d) Von-Mises stress is shown in Fig. 12. Column (d) represents the Von-Mises stresses in the different samples with colored contours. As can be seen clearly in Fig. 12, at the beginning of the analysis, stress concentration is mainly affected at the bottom-flange of beam by the internal forces, including bending moment and axial tension force in all connections. As the analysis continued and transitioned from the bending phase to the catenary action phase and with increase in axial tension forces, various components of the sample structure have participated in the significant load transfer, with a nonlinear behavior observed in most of the different areas of the beam. With increasing displacement, in the load transfer path from the removed column to the beam, at large displacements, the connection bolts have been subjected to stresses where this load is not considered in the design stage of the various elements. As the analytical process continues, various areas of the beam are buckling, with the connection bolts fractured one after the other with displacement elevation according to the control-displacement analysis. Note that in various connections where no stiffener is installed in the beam flanges, at large displacements, the buckling in the bottom-flange and the beam web is occurring under tension. With fracture of the bolts, rupture is also observed at the bottom-flange of beam near the end plate. However, in the connections where a stiffener is installed on the beam flanges, there is no buckling in the bottom-flange of beam, and its buckling occurs in the beam web and top-flange where the stiffener is ended. In this case, the rupture in the stiffener attached to the bottom flange is visible in addition to the fracture of the bolts. Thus, the failure mode of sample structures changes depending on the use or non-use of stiffeners in the beam flanges. Thus, the capacity and ductility of the sample vary according to the results presented in Table 3. The notable point is that in the proposed 10-B/U connection, fracture has only occurred in the bolts while the various components of the beam are not buckling. This suggests that the bolt arrangement can be very effective in the resistance of the connection against progressive collapse.

The stress-displacement diagram of the sample structure in the top and bottom-flange of beam is shown in Fig. 13 comparatively for eight different types of connections at the

beam-to-column connection 5 cm away from the column face. According to Fig. 13a, the top-flange of beam in all connections has been under compressive stresses before the fracture of the bolts around the bottom flange has occurred. With increase in the displacement and development of the catenary action mode, the compressive stresses on the top flange began to decrease. The bottom-flange of beam, which fracture of the bolts started at all connections in this region with displacement increasing, is located under tensile stress during all stages of analysis. Among all investigated connections, the highest stresses were recorded in the 16B (d16) connection. Connections which the stiffener installed on the beam flanges experienced more stresses than the connections without stiffener, where these connections had the best performance owing to removing the critical stresses from the connection region. The 6B/U connection with early fracture and tolerance of very low stresses and vertical load lower than the other connections demonstrated the weakest performance against progressive collapse. As shown in Fig. 13b, the bottom-flange of beam withstood the tensile stresses at all stages of analysis. On the other hand, according to Fig. 13a, in non-stiffened connections after fracture of bolts, the compressive stresses in the top-flange of beam diminished and the tensile stresses occurred partially in this flange.

5 Conclusion

When a progressive collapse occurred due to column removal, the connections of the beam-to-column structure must have sufficient strength and be able to bridge over the removed column. Since prequalified connections are the primary connections used in steel structures with steel moment frames, the exact evaluation of the failure and reinforcement of these connections is essential. In this research, the resistance of a sample structure with a steel moment frame system and different kinds of beam-to-column connections against progressive collapse was evaluated via numerical finite element models.

The modeling of the samples was done with a composite of three columns and two beams with eight different types of connection. The quasi-static nonlinear analysis was used to perform numerical simulations, with the numerical model verification performed against experimental results. The significant results of this research within the range of studied models are:

- The overall failure of the samples occurred in the connection region under the catenary action mode at large displacements. In this case, the performance of the structure changed from bending to the catenary, and

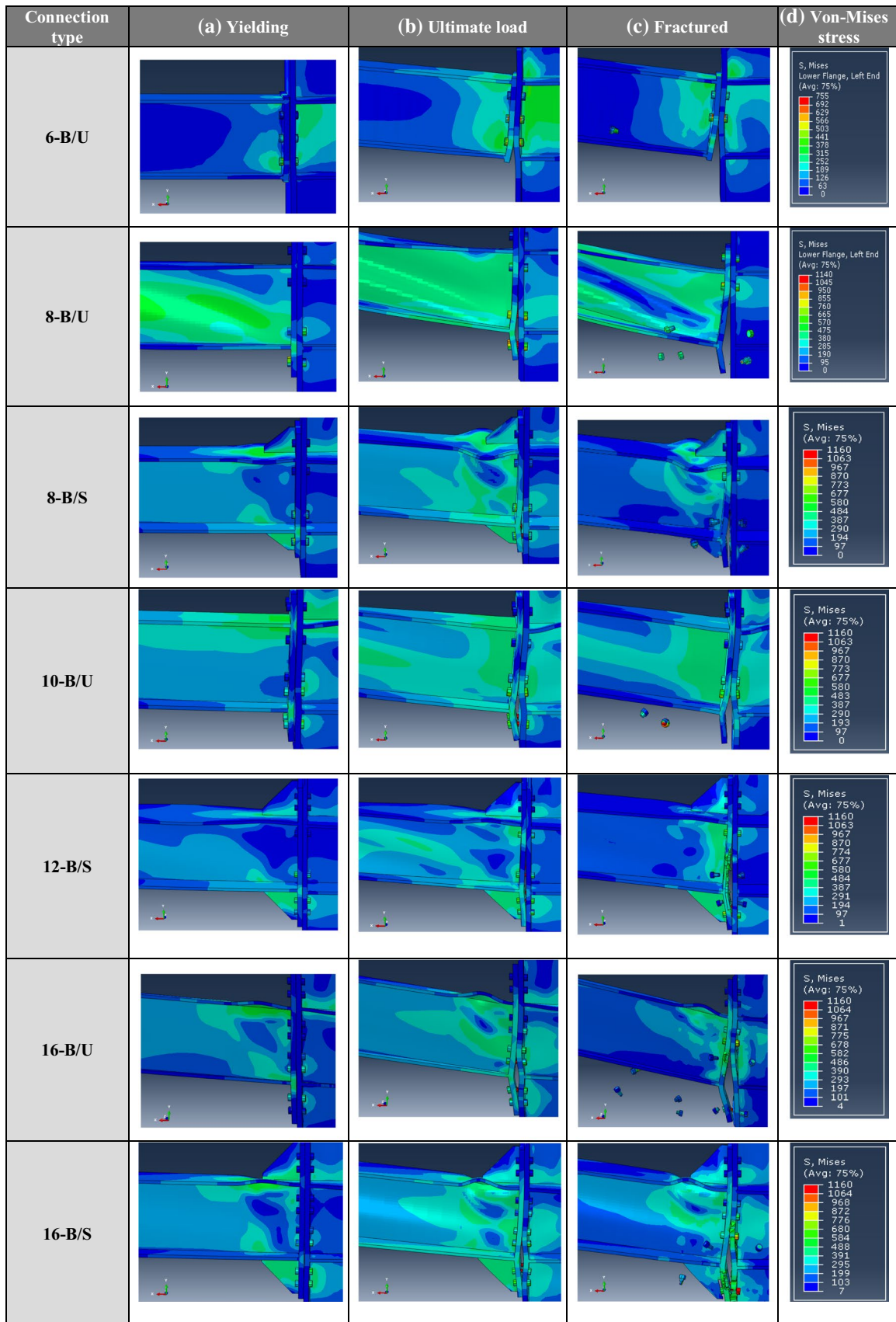
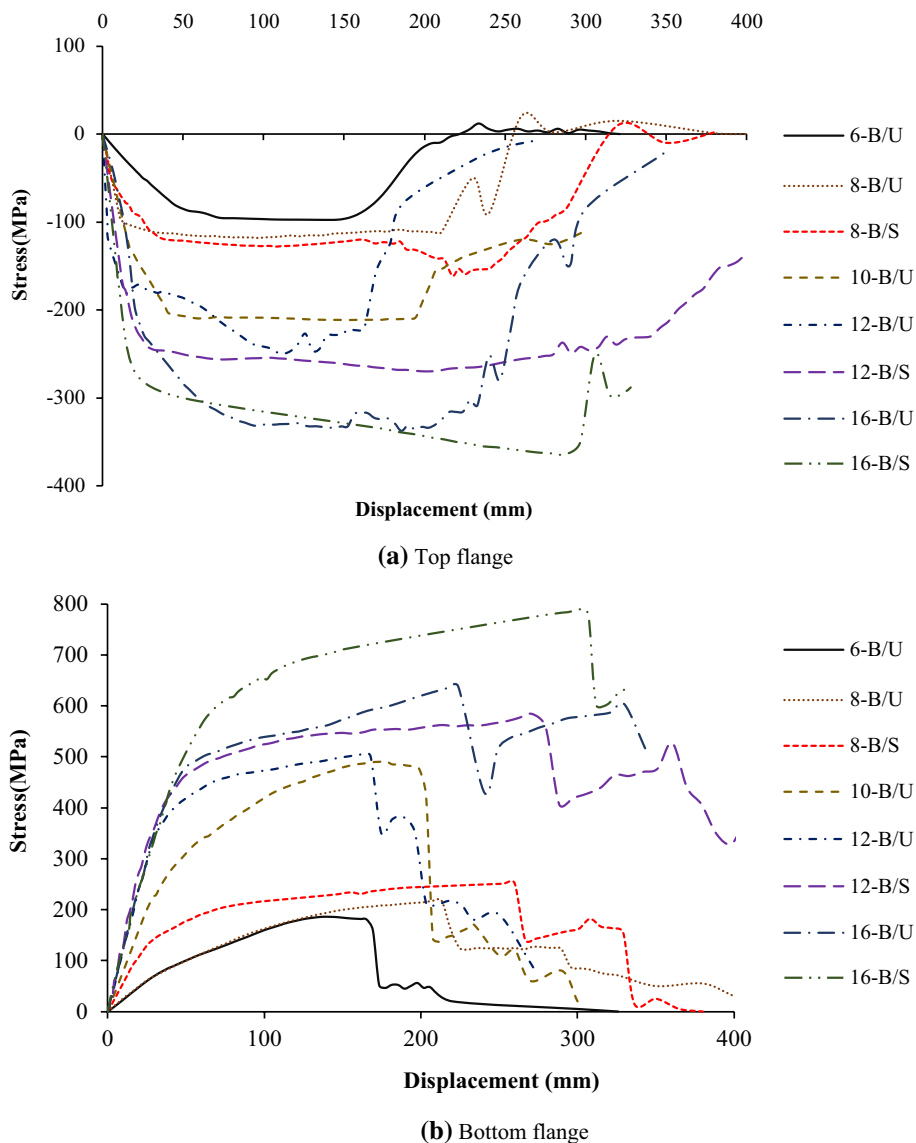


Fig. 12 Performance of various types of connections in different steps of the progressive collapse analysis

Fig. 13 Stress-displacement curve of the different connections



a considerable tensile axial force was generated in the sample developing the failure mode.

- Since the design of the connection is only based on the internal forces, including bending moment and shear force caused by gravity and seismic loads, in the design of buildings exposed to unusual loads due to the phenomenon of progressive collapse, the significant axial force created in the connections should be considered in the design stages of these elements.
- Among all investigated connections, the highest stresses were applied to the 16-B/S connection, and among all samples, this connection offered the best performance.
- The 6-B/U connection with early fracture and tolerance of very low stresses and vertical load below the other connections demonstrated the weakest performance against progressive collapse.
- In the seismic design, increasing the number of bolts and reducing the bolt size in the end-plate connections are directly interrelated. However, in the anti-progressive collapse design by adding a row of the bolt in the bottom-flange of beam, the load transfer paths increase, thereby significantly enhancing the ductility and structural capacity against this phenomenon. In other words, by increasing the bolt number in the bottom flanges, practically the resistance to the prying action grows under the tension due to catenary action; and because of this, the strength of connection increases.
- Since a more desirable performance of the sample structure was achieved by adding a row of bolts around the bottom-flange of beam in the end-plate connection, it is recommended that at least three rows of bolts are considered in the bottom area of these connections when the structure is at risk of progressive collapse.

- In the end-plate connections stiffened in the beam flanges, due to the removal of critical stress from the connection region, the performance of the sample improved as compared to the non-stiffened mode. In such as case, the sample would withstand more stresses and offer higher ductility under progressive collapse, with the failure mode manifested by the fracture of the bolts around the bottom-flange of beam along with the lower stiffener rupture. In these connections, no buckling occurred in the bottom-flange of beam, while the local buckling occurred on the beam web and top-flange where the stiffener ended.
- In the non-stiffened end-plate connections with different numbers of bolts, the failure mode was fixed, where this mode appeared as a failure in the bolts around the bottom-flange of beam. In these connections, there is always a buckling in the beam web and bottom-flange.

References

- ABAQUS. (2014). *Analysis user's manual*. version 6.14, ABAQUS Inc.
- American Institute of Steel Construction (AISC). (2016a). *Seismic provisions for structural steel buildings*. ANSI/AISC 341, Chicago, IL.
- American Institute of Steel Construction (AISC). (2016b). *Specification for structural steel buildings*. ANSI/AISC 360–16, Chicago, IL.
- American Institute of Steel Construction (AISC). (2016c). *Prequalified connections for special and intermediate steel moment frames for seismic applications*. ANSI/AISC 538, Chicago, IL.
- American Society of Civil Engineers (ASCE). (2016). *Minimum design loads for buildings and other structures*. ASCE7–16, New York.
- American Society for Testing and Materials (ASTM). (2018). *Standard test methods and definitions for mechanical testing of steel products*. ASTM A370, West Conshohocken, PA.
- Astaneh-Asl, A., Jones, B. & Zhao, Y. (2001). *Progressive collapse resistance of steel building floors*. UCB/CEE-STEEL-2001/03, University of California at Berkeley.
- Brett, C., & Lu, Y. (2013). Assessment of robustness of structures: Current state of research. *Frontiers of Structural and Civil Engineering*, 7(4), 1–13.
- Ch-Salmasi, A., & Sheidaii, M. R. (2017). Assessment of eccentrically braced frames strength against progressive collapse. *International Journal of Steel Structures*, 17(2), 543–551.
- Daneshvar, H. (2013). *One side steel shear connection in column removal scenario*. UCB/CEE-STEEL-2013/07, University of Alberta.
- Fang, C., Izzuddin, B. A., Obiala, R., Elghazouli, A. Y., & Nethercot, D. A. (2012). Robustness of multi-storey car parks under vehicle fire. *Journal of Constructional Steel Research*, 75(1), 72–84.
- Fang, C., Izzuddin, B. A., Elghazouli, A. Y., & Nethercot, D. A. (2013). Simplified energy-based robustness assessment for steel-composite car parks under vehicle fire. *Engineering Structure*, 49(1), 719–732.
- Lew, H. S., Main, J. A., Robert, S. D., Sadek, F., & Chiarito, V. P. (2013). Performance of steel moment connections under a column removal scenario. I: Experiments. *Journal of Structural Engineering*, 139(1), 98–107.
- Li, L., Wang, W., Chen, Y., & Lu, Y. (2013). Experimental investigation of beam-to-tubular column moment connections under column removal scenario. *Journal of Constructional Steel Research*, 88(9), 244–255.
- Li, L., Wang, W., Chen, Y., & Lu, Y. (2015). Effect of beam web bolt arrangement on catenary behaviour of moment connections. *Journal of Constructional Steel Research*, 104(1), 22–36.
- Meng, B., Zhong, W., & Hao, J. (2018). Anti-collapse performances of steel beam-to-column assemblies with different span ratios. *Journal of Constructional Steel Research*, 140(1), 125–138.
- National Institute of Science and Technology (NIST). (2005). *Final report on the collapse of the world trade center towers*. NCSTAR 1, US Department of Commerce, Gaithersburg, Maryland.
- Qin, X., Wang, W., Chen, Y., & Bao, Y. (2015). Experimental study of through diaphragm connection types under a column removal scenario. *Journal of Constructional Steel Research*, 112(9), 293–304.
- Qin, X., Wang, W., Chen, Y., & Bao, Y. (2016). A special reinforcing technique to improve resistance of beam-to-tubular column connections for progressive collapse prevention. *Engineering Structures*, 117(1), 26–39.
- Sadek, F., Main, J. A., Lew, H. S., & Bao, Y. (2011). Testing and analysis of steel and concrete beam-column assemblies under a column removal scenario. *Journal of Structural Engineering*, 137(9), 881–892.
- Sadek, F., Main, J. A., Lew, H. S., & El-Tawil, S. (2013). Performance of steel moment connections under a column removal scenario. II: analysis. *Journal of Structural Engineering*, 139(1), 108–119.
- Sadek, F., Main, J. A., Lew, H. S., Robert, S. D., Chiarito, V. P., & El-Tawil, S. (2010). An experimental and computational study of steel moment connections under a column removal scenario. *NIST Technical Note 1669*, National Institute of Standards and Technology, Maryland.
- The U.S. General Service Administration (GSA). (2013). *Progressive collapse analysis and design guidelines for new federal office buildings and major modernization projects*. Washington, D.C.
- Unified facility criteria (UFC). (2016). *Design of building to resist progressive collapse*. Department of Defense (DOD), Washington, D.C.
- Wang, W., Fang, C., Qin, X., Chen, Y., & Li, L. (2016). Performance of practical beam-to-SHS column connections against progressive collapse. *Engineering Structures*, 106(1), 332–347.
- Yang, B., & Tan, K. H. (2012a). Numerical analyses of steel beam-column joints subjected to catenary action. *Journal of Constructional Steel Research*, 70(3), 1–11.
- Yang, B., & Tan, K. H. (2012b). Robustness of bolted-angle connections against progressive collapse: experimental tests of beam-column joints and development of component-based models. *Journal of Structural Engineering*, 139(9), 1498–1514.
- Yang, B., & Tan, K. H. (2013). Experimental tests of different types of bolted steel beam-column joints under a central-column-removal scenario. *Engineering Structures*, 54, 112–130.
- Zhong, W., Meng, B., & Hao, J. (2017). Performance of different stiffness connections against progressive collapse. *Journal of Constructional Steel Research*, 135, 162–175.

Publisher's Note Springer Nature remains neutral with regard to jurisdictional claims in published maps and institutional affiliations.